

Periodic pillar structures by Si etching of multilayer GeSi/Si islands

Z. Zhong,^{a)} G. Katsaros, M. Stoffel, G. Costantini, K. Kern, and O. G. Schmidt
Max-Planck-Institut für Festkörperforschung, Heisenbergstr. 1, D-70569 Stuttgart, Germany

N. Y. Jin-Phillipp
Max-Planck-Institut für Metallforschung, Heisenbergstr. 3, D-70569 Stuttgart, Germany

G. Bauer
Institute for Semiconductor Physics, Johannes Kepler University Linz, A-4040 Linz, Austria

(Received 14 June 2005; accepted 8 November 2005; published online 21 December 2005)

Laterally aligned multilayer GeSi/Si islands grown on a patterned Si (001) substrate are disclosed by selective etching of Si in a KOH solution. This procedure allows us to visualize the vertical alignment of the islands in a three-dimensional perspective. Our technique reveals that partly coalesced double islands in the initial layer do not merge together, but instead gradually reproduce into well-separated double islands in upper layers. We attribute this effect to very thin spacer layers, which efficiently transfer the strain modulation of each island through the spacer layer to the surface. The etching rate of Si is reduced in tensile strained regions, which helps to preserve sufficient Si between the stacked islands to form a periodic array of freestanding and vertically modulated heterostructure pillars. © 2005 American Institute of Physics.

[DOI: 10.1063/1.2150278]

Self-assembled GeSi islands grown via the Stranski-Krastanov mode on Si(001) substrates have been widely investigated during the last decade. The interest is mainly driven by their promising applications in a new generation of devices compatible with the existing Si technology¹ and by the understanding of strained layer epitaxy.² In particular, the growth of multilayers consisting of self-assembled islands separated by spacer layers has been thoroughly studied³⁻¹² since such heterostructures provide a way to increase the island density, which is of fundamental importance for device applications.^{3,4} An additional benefit of multilayer islands is the improvement of the lateral ordering and the size homogeneity of the islands in upper layers.⁵ By growing multilayer islands on patterned Si (001) substrates, three dimensionally ordered islands (quantum dot crystals) have been realized, and characterized by cross-sectional transmission electron microscopy (XTEM) and x-ray diffraction.¹⁰ Selective etching is used to investigate the compositional state of self-assembled islands and the formation processes of single- and multiple-island layers.¹²⁻¹⁵

In this letter, we investigate the Si etching of multilayers consisting of GeSi islands separated by thin Si spacers grown on a prepatterned Si(001) substrate. A periodic array of vertical stacks of GeSi/Si islands is clearly disclosed and imaged in three dimensions by scanning electron microscopy (SEM) and XTEM. We find that some laterally closely spaced islands, which are in contact at their base, do not merge together during stacking but, instead, gradually develop into well-separated double islands in upper layers. Furthermore, we find that tensile strained Si regions are etched slower than bulk unstrained Si. Thus, a substantial part of the Si spacer layers remains unaffected, and modulated pillar structures can form during etching. The lateral ordering of these pillar structures, possibly enable the fabrication of a two-dimensional (2D) photonic crystal.¹⁶

The investigated samples were grown by solid-source molecular-beam epitaxy on prepatterned Si(001) substrates. A pattern consisting of a regular array of pits having a depth of ~ 28 nm and periodicities of ~ 400 nm along two orthogonal $\langle 110 \rangle$ directions was fabricated by holographic lithography¹⁷ and subsequent reactive ion etching. After cleaning and oxide desorption, the layer structure shown in 1(a) was grown. The growth rate of Si and Ge are about 0.5 \AA/s and 0.04 \AA/s , respectively. At the growth temperatures used, Si intermixing already occurs and consequently, GeSi islands form.¹⁵ The morphology of the sample before

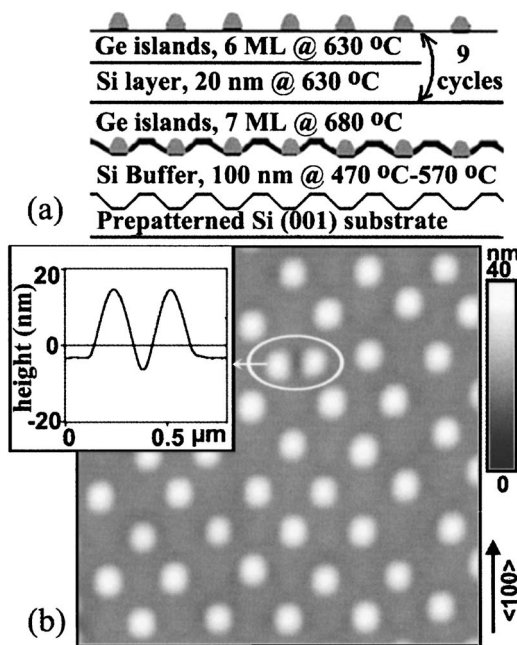


FIG. 1. (a) Schematic illustration of the sample structure, and (b) AFM image ($3 \times 3 \mu\text{m}^2$) of the sample morphology before KOH etching. The white ellipse identifies a double-island defect. The inset shows a height profile across the marked doubled islands.

^{a)}Also at: Institute for Semiconductor Physics, Johannes Kepler University Linz, A-4040 Linz, Austria; electronic mail: zhenyang.zhong@jku.at

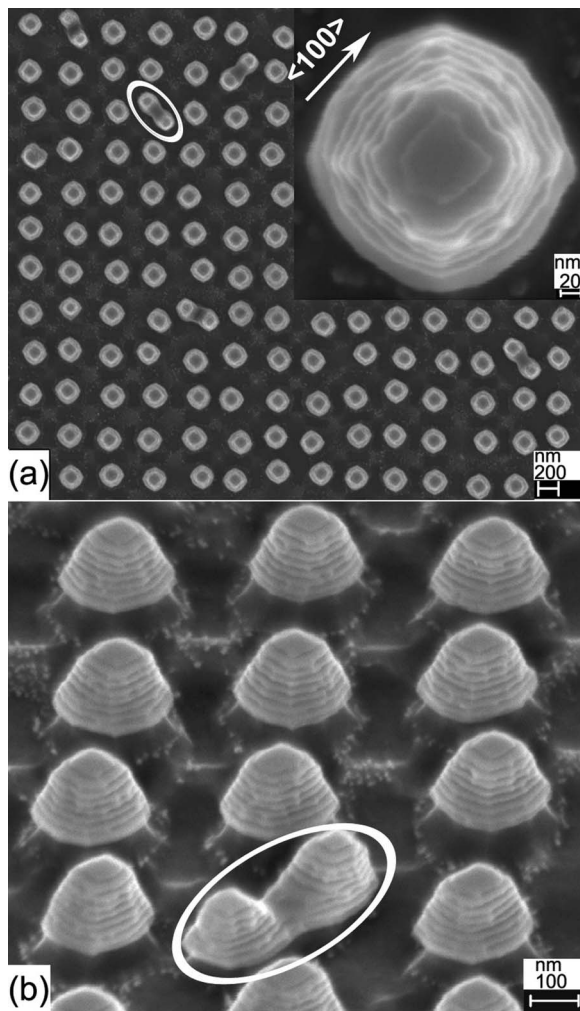


FIG. 2. SEM image of the sample after KOH etching (a) top view, and (b) top-side view. The inset in (a) shows the zoomed-in top view of a single pillar structure. The ellipse in (a) and (b) indicates the double closely spaced pillar structure.

etching was measured by a Digital Instruments atomic force microscope in tapping mode. The sample was etched *ex situ* by a 2 mol/liter KOH solution at room temperature for about 15 min. The SEM images were obtained by a Zeiss Cross-Beam® 1540XB apparatus, which was also used to prepare TEM specimens with a $\{110\}$ cross section. The TEM was performed in a Philips CM200 microscope operated at 200 kV.

The surface morphology of the sample before etching is shown in Fig. 1(b). As reported previously,¹⁰ well-ordered islands aligned along $\langle 110 \rangle$ directions can clearly be observed. Their average height and diameter is about 19 nm and 260 nm, respectively. We can, however, identify some islands, which are not exactly located at square lattice positions. When the bottom area of the pit is sufficiently large, islands can form at one particular corner. As a result, some islands are not located exactly at the center of the pit and the ordering is not perfect. At certain sites, we can also identify the formation of two closely spaced islands predominantly oriented along $\langle 100 \rangle$ directions, as denoted by the white ellipse in Fig. 1(b). A cross-sectional profile along the axis of the double islands is shown in the inset of Fig. 1(b). Such double islands already form in the first layer of the island stack as shown in Fig. 2(b). It has been found previously that

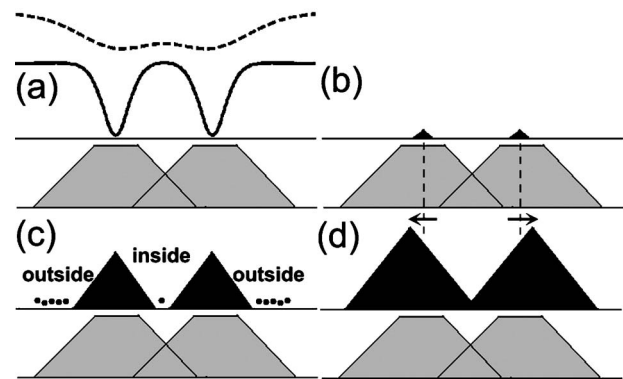


FIG. 3. Schematic illustration of the growth of closely spaced double islands: (a) Spatial distribution of the local chemical potential after the growth of thick (dotted line) and thin (solid line) spacer layer, (b) formation of the double islands, (c) growth of the double islands, the solid black circles represent adatoms, and (d) fully developed double islands.

patterned pits have the shape of inverted truncated pyramids with edges aligned along $\langle 110 \rangle$ directions after Si buffer layer growth.¹⁷ If the bottom area of the pit is too large, two (or even more) islands can form at the bottom corners, preferentially along the diagonal $\langle 100 \rangle$ directions.¹⁸ If the Si spacer is sufficiently thin, the double islands in the initial layer replicate themselves in stacked layers leading to the morphology observed in Fig. 1(b).

Figure 2(a) shows a top-view SEM image obtained after selective etching of the sample shown in Fig. 1(b) in a KOH solution. We can identify well-ordered pillar structures which correspond to the stacked GeSi islands. Each individual island layer can be clearly resolved since the lateral sizes of the islands in the stack systematically increase from top to bottom, as shown in the top-view image of a magnified single pillar [inset of Fig. 2(a)] and in the inclined view of the pillars [Fig. 2(b)]. This is due to the fact that parts of the GeSi islands are also etched by KOH. Since the different island layers are successively exposed to the KOH solution, an increased island volume in the upper layers will be etched away due to a longer etching time. For the same reason, most of the pillars contain only nine island layers although the nominal structure before etching contains ten layers. The three-dimensional (3D) view of the island stacks in Fig. 2 reveals further that the island centers are aligned along the growth direction. This demonstrates that the islands are originally vertically aligned in the Si matrix.

At certain sites, we also identify several closely spaced double-pillar structures, as marked by white ellipses in Fig. 2. The double pillars originate from double-island formation in large bottom area pits, as discussed above. Since the lateral size of each of the double islands is larger than the distance between them, the islands are in contact at their bases as revealed by the structure of the region separating the double pillars. The replication of double islands in successive layers, which is in contrast to the previously observed coalescence,⁷ can be explained as follows: The buried islands generate on top of the thin Si spacer layers two well-separated local chemical potential minima,^{5,6} as schematically shown (solid line) in the upper panel of Fig. 3(a). Thus, the new islands can form right above the buried double ones as shown in Fig. 3(b). Furthermore, since the size of the double islands increases in the upper layers, the region located in between them becomes increasingly compressed and

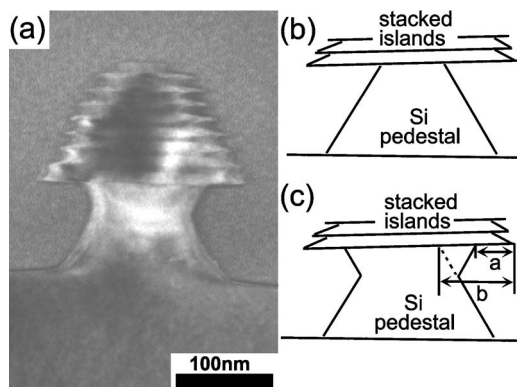


FIG. 4. (a) XTEM image of a pillar structure after KOH etching. (b) and (c) Schematic profiles of pillar structures after KOH etching without and with the effect of tensile strain on the Si etching rate, respectively.

therefore unfavorable for Ge (Si) adatoms. As a result, much less Ge (Si) adatoms stay in between the islands, as schematically shown in Fig. 3(c) (“inside” region). Accordingly, the centers of the new double islands can be slightly shifted in opposite directions during growth, as schematically shown by the arrows in Fig. 3(d). Consequently, partly coalesced double islands in the initial layer gradually develop into two well-separated double islands in the upper layers. Indeed, the line scan shown in the inset of Fig. 1(b) clearly demonstrates that in the tenth layer, both islands are not connected. The region located in between the double pillars is highly strained. This may affect the migration of Si and Ge atoms, most probably to some different degree. However, the Ge distribution within the double pillars is not considerably modified. Consequently, the etching rates are almost the same on both pillar sides and no clear asymmetry can thus be observed.

After KOH etching, the island edges tend to align along $\langle 100 \rangle$ directions, as shown in the inset of Fig. 2(a). One possible reason could be the anisotropy of the GeSi etching rate, which is smaller along $\langle 100 \rangle$ directions than along, e.g., $\langle 110 \rangle$ directions, similarly to Si.¹⁹ The irregularities at the island edges may be due to the thinning of the edges. However, high-resolution TEM characterizations (not shown here) confirm that these pillars are still crystalline.

Figure 4(a) shows a TEM image of a single-pillar structure. Due to the long etching time, in addition to the disclosed island stack, underetching of the Si substrate occurs, resulting in a mushroomlike shape. Considering the anisotropy of the etching rate,¹⁹ we would expect a monotonic increase of the lateral size of the Si pedestal when moving toward the substrate due to a reduced etching time, as schematically shown in Fig. 4(b). However, this is not observed experimentally. Instead, the region located directly below the island stack is etched much slower than the bottom of the pedestal. The reduction of the Si etching rate may result from a slower diffusion of ions below the island stack or may be caused by the tensile strain extending below the island.²⁰ The first hypothesis can be ruled out since the same pedestal shape was observed for longer etching times. The etching rate reduction may be estimated from the ratio a/b , as shown in Fig. 4(c). In our case, the ratio is close to 0.6. The slower etching rate of tensile-strained Si may also be responsible for

the stability of the free-standing GeSi/Si pillars.

We expect that the pillar structures can be further optimized. In order to compensate for the GeSi etching in the upper layers due to a longer exposure time, the size of islands should be increased, e.g., by gradually increasing the amount of deposited Ge with increasing layer number. In that case, more island layers may be grown to obtain higher pillars after etching. Moreover, by optimizing the etching conditions,¹⁹ higher pillar aspect ratios may be obtained. The growth conditions can also be further optimized to yield perfectly ordered islands and thus perfectly periodic pillar structures. Such structures may act as a 2D photonic crystal,¹⁶ which could possibly be integrated with other island-based devices on a same Si(001) substrate.

In summary, 3D ordered GeSi island stacks were obtained by growing multilayer islands on a patterned Si(001) substrate. By selectively etching Si in a KOH solution, periodic pillar structures were obtained. The characterizations of the pillar structures reveal that they are composed of stacked GeSi/Si islands and a Si pedestal. The vertical alignment and evolution of single and double islands during multilayer growth are visualized in a 3D perspective way and qualitatively discussed. We further found that the etching rate of Si by KOH is strain sensitive.

The authors thank A. Schertel for TEM sample preparation. This work was supported by the BMBF (03N8711) and the EU NOE SANDiE.

¹O. G. Schmidt and K. Eberl, IEEE Trans. Electron Devices **48**, 1175 (2001).

²J. Stangl, V. Holy, and G. Bauer, Rev. Mod. Phys. **76**, 725 (2004).

³J. L. Liu, W. G. Wu, A. Balandin, G. L. Jin, and K. L. Wang, Appl. Phys. Lett. **74**, 185 (1999).

⁴A. I. Yakimov, A. V. Dvurechenskii, A. I. Nikiforov, and Y. Y. Proskuryakov, J. Appl. Phys. **89**, 5676 (2001).

⁵J. Tersoff, C. Teichert, and M. G. Lagally, Phys. Rev. Lett. **76**, 1675 (1996).

⁶Q. Xie, A. Madhukar, P. Chen, and N. P. Kobayashi, Phys. Rev. Lett. **75**, 2542 (1995).

⁷E. Mateeva, P. Sutter, J. C. Bean, and M. G. Lagally, Appl. Phys. Lett. **71**, 3233 (1997).

⁸O. Kienzle, F. Ernst, M. Rühle, O. G. Schmidt, and K. Eberl, Appl. Phys. Lett. **74**, 269 (1999).

⁹O. G. Schmidt and K. Eberl, Phys. Rev. B **61**, 13721 (2000).

¹⁰Z. Zhong, G. Chen, J. Stangl, T. Fromherz, F. Schäffler, and G. Bauer, Physica E (Amsterdam) **21**, 588 (2004).

¹¹O. Kermarrec, Y. Campidelli, and D. Bensahel, J. Appl. Phys. **96**, 6175 (2004).

¹²O. G. Schmidt, U. Denker, S. Christiansen, and F. Ernst, Appl. Phys. Lett. **81**, 2614 (2002).

¹³Z. M. Wang, L. Zhang, K. Holmes, and G. J. Salamo, Appl. Phys. Lett. **86**, 143106 (2005).

¹⁴U. Denker, M. Stoffel, and O. G. Schmidt, Phys. Rev. Lett. **90**, 196102 (2003).

¹⁵T. U. Schullli, M. Stoffel, A. Hesse, J. Stangl, R. T. Lechner, E. Wintersberger, M. Sztucki, T. H. Metzger, O. G. Schmidt, and G. Bauer, Phys. Rev. B **71**, 035326 (2005).

¹⁶S. Assefa, P. T. Rakich, P. Bienstman, S. G. Johnson, G. S. Petrich, J. D. Joannopoulos, L. A. Kolodziejski, E. P. Ippen, and H. I. Smith, Appl. Phys. Lett. **85**, 6110 (2004).

¹⁷Z. Zhong and G. Bauer, Appl. Phys. Lett. **84**, 1922 (2004).

¹⁸J. Zhu, K. Brunner, and G. Abstreiter, Appl. Phys. Lett. **73**, 620 (1998).

¹⁹K. Sato, M. Shikida, Y. Matsushima, T. Yamashiro, K. Asaumi, Y. Iriye, and M. Yamamoto, Sens. Actuators, A **64**, 87 (1998).

²⁰D. T. Tambe and V. B. Shenoy, Appl. Phys. Lett. **85**, 1586 (2004).